

SERS-Based Lateral Flow Assay for Sensitive Detection of Troponin-I via Core-Shell Plasmonic Nanoparticles [†]

Insu Kim, Eunyeong Song, Changsu Jeon and Sunghyun Pyun *

R&D Center, Speclipse Inc., Seongnam 13461, Republic of Korea; insukim@speclipse.com (I.K.); eunyeong.song@speclipse.com (E.S.); csu.jeon@speclipse.com (C.J.)

* Correspondence: sunghyun.pyun@speclipse.com

[†] Presented at the 3rd International Electronic Conference on Biosensors, 8–21 May 2023; Available online: <https://iecb2023.sciforum.net>.

Abstract: A highly sensitive quantification of cardiac troponin I (cTnI) immunochromatographic assay (ICA) is challenging because the reference range of cTnI in adults is far lower than the detection limits of ICA. Here, we present a highly sensitive POC platform, a surface-enhanced Raman spectroscopy-based immunochromatographic assay (SERS-ICA) for the detection of cTnI. By taking advantage of core-shell structured plasmonic nanoparticles, Raman scattering and free surface area were maximized, which improves the sensing performance. Consequently, the detection limits of SERS-ICA increased at least 100-fold to conventional ICA. Selectivity of SERS-ICA to cTnI was also verified against other AMI biomarkers. Finally, the cTnI-spiked in human serum was measured with proposed platform that the result highly correlate to measurement in PBS.

Keywords: cardiac troponin i; surface-enhanced raman spectroscopy (SERS); immunochromatographic assay (ICA); plasmonic nanoparticle

1. Introduction

Acute myocardial infarction (AMI), one of the important cardiovascular diseases (CVDs), raises a concern for public health [1]. AMI occurs for various reasons related to the blockage in one of the blood vessels supplies to the heart, mostly caused by plaque [2].

Several biomarkers, related to determining the presence of myocardial necrosis, were reported to diagnose AMI such as cardiac troponins, creatine kinase MB (Ck-MB), myoglobin (Myo), and myeloperoxidase [3]. Among them, a blood test of cardiac troponin-I (cTnI) was clinically well-verified for AMI diagnosis that they have superior sensitivity and specificity for determining myocardial necrosis [4–6]. Also, cTnI level showed the most rapid elevation than other biomarkers when myocardial necrosis occurs, which is one of the most critical factors for life-saving from AMI.

To date, various bio-transducers were reported for cTnI detection such as electrochemical, optical, electronic, piezoelectric, galvanic, and magnetic transducers [7–9]. There are some conditions that make cTnI sensors more applicable and practical considering the urgency of the life-threatening disease. Several important conditions are as follows; POC platform, easy to use with minimum pretreatments of sample, rapid read out, and enough sensitivity for reference range of cTnI. During the COVID-19 pandemic, paper-based ICA, also called lateral flow assay, was a powerful tool for determining the infection within an hour. The main components of ICA are nitrocellulose membranes as a fluidic channel, antibody pairs for sandwich immunoassay, and gold nanoparticles for transducing immune reaction to optical signal. Unlike the determination of virus, however, it is necessary to quantify the concentration of cTnI. It is possible to quantify the target protein in ICA by using CCD camera and optical analysis [10,11]. The detection limit of optical analysis of ICA is reported to be single-digit nanogram level, which can

Citation: Kim, I.; Song, E.; Jeon, C.; Pyun, S. SERS-Based Lateral Flow Assay for Sensitive Detection of Troponin-I via Core-Shell Plasmonic Nanoparticles. *Eng. Proc.* **2023**, *5*, x. <https://doi.org/10.3390/xxxxx>

Academic Editor(s):

Published: 8 May 2023



Copyright: © 2023 by the authors. Submitted for possible open access publication under the terms and conditions of the Creative Commons Attribution (CC BY) license (<https://creativecommons.org/licenses/by/4.0/>).

distinguish emergence patients, yet insufficient to sub-nano level. To overcome the sensitivity of optical analysis of ICA, surface-enhanced Raman spectroscopy (SERS) can be adapted to ICA (SERS-ICA).

SERS is a surface-sensitive analytical technique that enhances Raman scattering of the molecules adsorbed on the surface of noble metal such as gold and silver nanoparticles. In this regard, SERS tags, Raman reporter-labelled nanoparticles, are compatible with the gold nanoparticles used to ICA. It is reported that the gold nanoparticle itself can be utilized as a SERS tags for ICA and showed good result [12]. To achieve sensitive SERS-ICA, however, it is required to maximize the Raman intensity of SERS tags, which means higher Raman intensity for the same particle density on the test line of ICA. Nanoparticles for ICA include detection antibodies on the outer surface of core-shell structured nanoparticles favorable because the free outer surface for Ab conjugation is needed.

In this study, we synthesized sensitive SERS tags composed of gold core, silver shells, MBA, PEG, and antibody. The SERS tag showed 2 times higher Raman intensity after shell formation. Detection limits of ICA was 1 ng/mL and that of SERS-ICA was 10 pg/mL. SERS-ICA also showed good selectivity to cTnI against AMI biomarkers in blood such as C-reactive protein (CRP), CK-MB, and Myo. Finally, cTnI solubilized in diluted human serum was quantified by the SERS-ICA.

2. Materials and Methods

2.1. Reagents

cTnI monoclonal antibody pairs for detection and capture were purchased from Hytest (RC4T21, Finland) and Genetex (GTX10226, USA), respectively. Human serum, Human cardiac troponin I (cTnI), tween-20, sodium citrate, tetrachloroauric acid (HAuCl_4), silver nitrate (AgNO_3), 4-Mercaptobenzoic acid (MBA), 10 \times phosphate-buffered saline (PBS, pH 7.4), bovine serum albumin (BSA), potassium phosphate monobasic, and sodium phosphate dibasic were purchased from Sigma-Aldrich (USA).

2.2. Synthesis and Surface Modification of SERS Tags

Gold seeds and gold core silver shell nanoparticles were synthesized by inversed Turkevich method and a modified seed growth method, respectively [13,14]. All glassware was washed with aqua regia and ethanol before synthesis. Briefly, 100 mL of 2.2 mM sodium citrate in a three-neck flask was stirred and heated at 130 °C for 15 min. 1 mL of 25 mM HAuCl_4 was added when the sodium citrate solution was initiated to boil. The synthesis of gold seed was indicated by the color shift to soft pink within 10 min. After 10 min of reaction, the solution was cooled to 70 °C. For the Ag shell growth, 0.5 mL of 100 mM AA and 0.5 mL of 100 mM AgNO_3 were serially added and incubated for 30 min

The SERS tags were prepared by adding 400 μL of 1 mM MBA, dissolved in ethanol, to 20 mL of Au@AgNP solution. The solution was stirred and incubated for 3 h at room temperature. An Ag shell was coated on MBA-labeled Au@AgNP by adding 10 μL of 100 mM AA and 10 μL of 100 mM AgNO_3 . For PEGylation, 20 μL of 1 mM HS-PEG-COOH was added. The solution was incubated for 2 h at room temperature and washed twice to remove unreacted molecules. For chemisorption of detection Ab, the carboxyl groups of the PEG were activated by adding 10 μL of 6 mM EDC and 10 μL of 10 mM sulfo-NHS for 1 mL of PEGylated NPs. Then, 5 μL of 1 mg/mL anti-TnI was added and reacted for 1 h. Next, ethanalamine was added to deactivate the unreacted sites. Finally, SERS tags were washed twice by centrifugation and stored at 4 °C.

2.3. Preparation of SERS-Immuno-chromatographic Assay (ICA) Strip

Test and control line was dispensed by contact dispenser with 2 mg/mL of anti-cTnI and 0.5 mg/mL of anti-mouse IgG, respectively. The thickness of the lines was about 0.5 mm following conditions; dispense rate of 0.4 $\mu\text{L}/\text{cm}$ and speed of 60 mm/s. Then, the

membrane was incubated at 37 °C for 2 h and cut with the width of 4 mm. For the storage, strips were sealed in a plastic bag containing silica gel and kept at room temperature.

2.4. Optical and SERS Analysis

Optical images were obtained by CCD sensor (ISOCELL HM3, Samsung, Korea) in a controlled set-up; a distance of 80 mm, shutter speed of 0.5 s, ISO 50, white balance of 3800K, and exposure value of 1.7. The images of ICA strips were analyzed using ImageJ software [15]. In a color channel split step, the blue channel was selected for the highest sensitivity against yellow-colored SERS Tags (Figure S1).

The Raman intensity of SERS tags was measured with Raman spectroscope (Xplora Plus, Horiba, Japan). Mapping of the test line in the area of $2000 \times 600 \mu\text{m}$ with interval of $100 \times 50 \mu\text{m}$, attaining 240 pixels with $5\times$ objective lens, 638 nm laser, and 10% of laser power. The rolling-ball algorithm was used for estimating background intensity of each SERS spectra.

2.5. Instrumentation

The UV-Vis spectra of nanoparticles were measured using spectrophotometer (Lambda465, PerkinElmer, Waltham, MA, USA). The hydrodynamic size of SERS tags was measured using a zeta potential analyzer (Nano S90, Malvern, UK). The morphology of SERS tags was analyzed using transmission electron microscope (TEM, JEM-2010, Jeol, Musashino, Japan). To compare the intensity measured by optical intensity, ImageJ software was applied. Raman intensity was measured using confocal Raman microscope (Xplora Plus, Horiba, Kyoto, Japan); grating of 1200 grooves per mm, monochromatic laser of 638 nm, optical microscope with a $5\times$ objective lens. The UV-Vis spectra of nanoparticles were measured using spectrophotometer (Lambda465, PerkinElmer, USA).

3. Results and Discussion

3.1. Principle of SERS-ICA

A SERS tag is schematically illustrated in Figure 1a. The Au seed was used as growth templet for Ag shell. Raman active molecules with a thiol group are encoded on the surface of Ag shell. Then another Ag shell is coated over Raman active molecules. As a result, free outer surface of Ag shell is PEGylated via silver-thiol bond. Finally, antibodies are attached on the carboxyl group on PEG via EDC/NHS coupling.

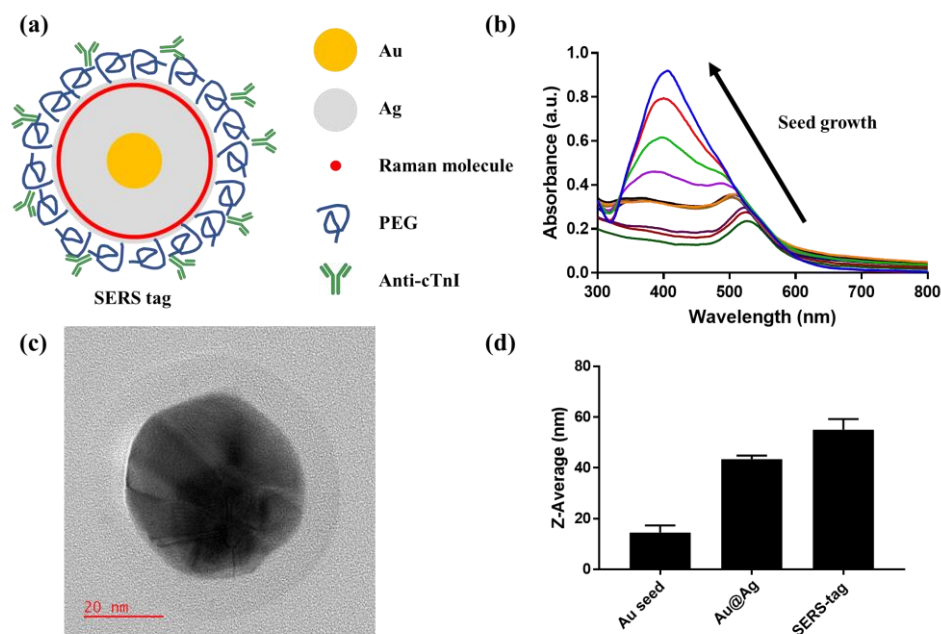


Figure 1. Characterization of SERS tags. (a) Schematic image of a SERS tag; (b) The UV-Vis spectra of each seed growth step of SERS tags; (c) TEM image of a SERS tag; (d) Hydrodynamic diameter of Au seeds, Ag coated Au seeds, and SERS tags.

3.2. Characterization of Ag SERS Tag

SERS tags were prepared via seed growth method. Au seeds with the diameter of 20 nm were synthesized using inverse Turkevich method. An Ag shell grew via 5 steps of AgNO_3 reduction through AA. As the step proceeded, the color of nanoparticles solution changed from red wine to orange, then finally to yellow, which indicates the Ag shell was fully thickened (Figure S2). It is reported that AgNPs showed stronger Raman Intensity than the same size of AuNPs [16]. The outer surface of Ag shell was coated with MBA for Raman signal. Then, another Ag shell was coated for free outer surface and Raman enhancement [14,17]. The Raman scattering of MBA existed on/in the gap between two Ag shells increased 50%. Also, the free outer surface was coated with SH-PEG-COOH for stabilization and chemical conjugation.

During the 6 steps of Ag shell growth, the absorbance spectra of nanoparticle were dramatically changed (Figure 1b). The peak wavelength of Au seeds was 525 nm and that of SERS tags was shifted to 410 nm. The change of peak wavelength indicates that the characteristics of silver become dominant over gold. Also, the maximum optical density of SERS tags was increased 3.9 times compared to the same number of Au seeds. As Ag shell grows, the size of particle increased and outer metal was changed to silver, which leads to the change of localized surface plasmon resonance (LSPR) which is a collective excitation mode of the plasma localized near the surface. It is well researched that LSPR is one of the most important factors for enhancing SERS intensity.

The electron microscopy images of Au seeds and SERS tags show actual diameters of each particle (Figure 1c). It is also discriminated that the Au seed as a core and silver coating as a shell by TEM.

The hydrodynamic diameter of Au seeds was 14.5 ± 2.8 nm. During six steps of Ag shell growth, the particle gradually increased to 43.4 ± 1.4 nm. (Figure 1d) After PEGylation, hydrodynamic diameter was largely increased to 55.1 ± 4.2 nm. The hydrodynamic diameter of NPs coated with macromolecules contains the radius of macromolecules.

After the fifth growth step, Raman reporter was coated on the outer surface of NPs by adding MBA and incubation (Au@AgNPs). Strong SERS peaks of MBA were shown at 1078 cm^{-1} and 1585 cm^{-1} (Figure S3). It is intriguing that the highest intensity was at 1585 cm^{-1} for 638 and 532 nm laser. On the other hand, the peak at 1078 cm^{-1} was the highest at 785 nm laser. As a result, the SERS peak at 1585 cm^{-1} using 638 nm laser was optimal for this system (Figure S4).

The MBA-labelled Au@AgNPs showed Raman intensity of 5517 ± 799 , and the intensity was increased 1.86 times after another Ag shell was coated to form SERS tags (Figure 2). The result was caused by LSPR increment.

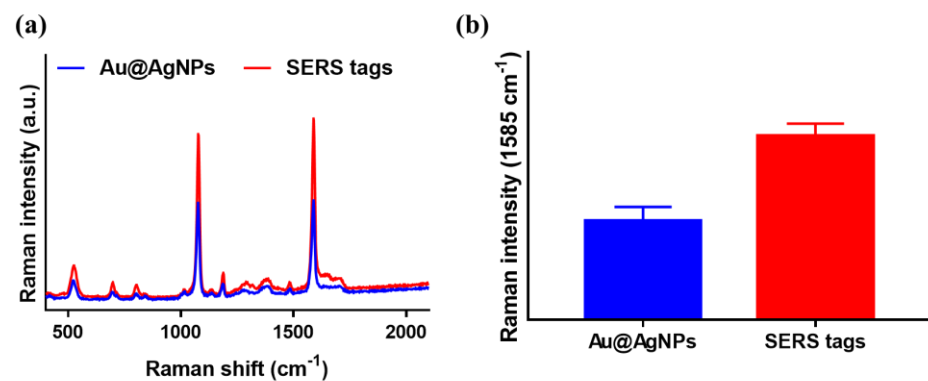


Figure 2. (a) Raman spectra of Au@AgNPs and SERS tags; (b) Raman intensity of Au@AgNPs and SERS tags.

3.3. Sensing Performance of cTnI in PBS via Optical and Raman Assay

The range of 0–100 ng/mL cTnI solubilized in PBS was measured by proposed SERS-ICA (Figure 3). The results from same strips were analyzed with optical and Raman analysis. It is obvious that cTnI of 1 ng/mL is a detection limit of sense of sight. Optical analysis also showed that the dynamic detection range is between 1–100 ng/mL, whereas, in Raman analysis, the dynamic detection range is between 0.01–100 ng/mL.

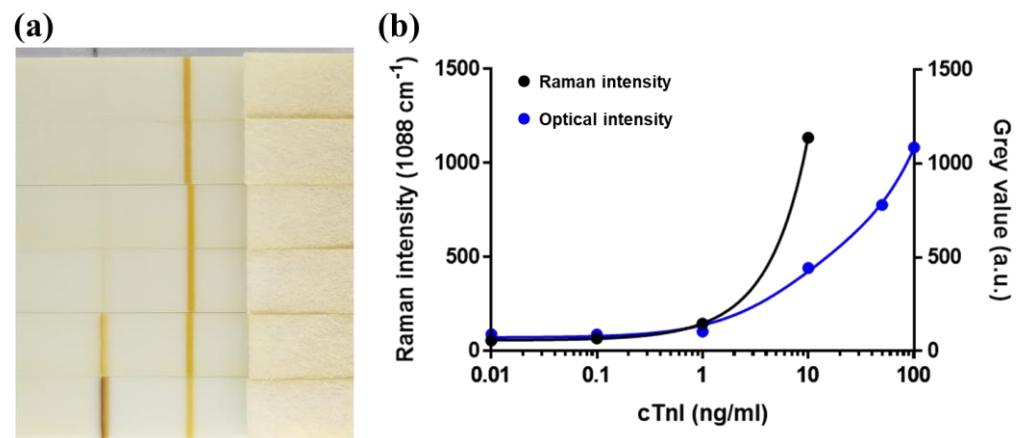


Figure 3. cTnI sensing performance of SERS-ICA. (a) Optical image of ICA strips of cTnI detection; (b) Optical and Raman analysis of the cTnI detection.

3.4. Selectivity and Human Serum Test

The selectivity of SERS-ICA was verified by testing 1000 ng/mL of CRP, Myo, and CK-MB against 1–100 ng/mL (Figure 4). It is verified that the Raman intensity of CRP, Myo, and CK-MB was negligible that the possible interference molecules barely different from blank. Also, the intensity of 1 ng/mL cTnI was 1.8–2.1 times higher than the molecules with 1000 times higher concentration. The intensity of 10 ng/mL cTnI was 6.4–7.2 times higher than the molecules with 100 times higher concentration.

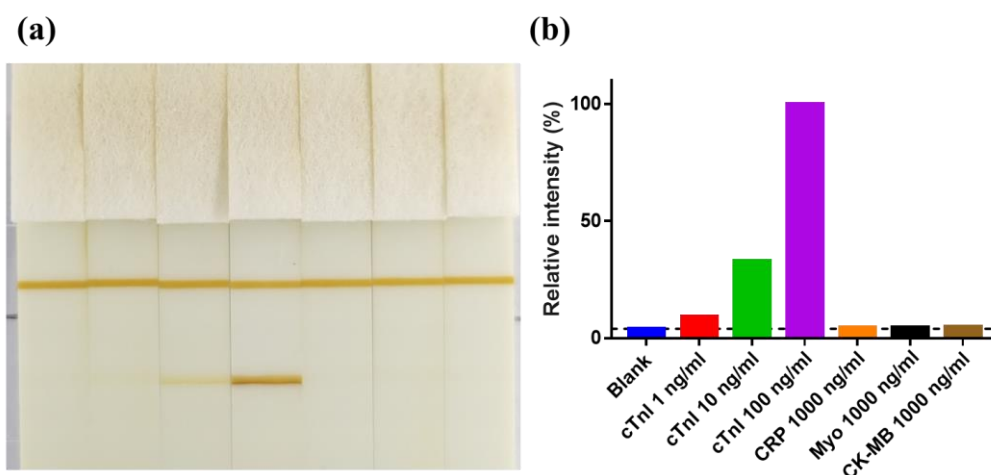


Figure 4. Selectivity of SERS-ICA. (a) Optical image of ICA strips of cTnI detection; (b) Optical and Raman analysis of the cTnI detection.

The sensing performance of SERS-ICA was validated measuring cTnI solubilized in 10-fold diluted human serum (Figure 5). The result was similar to the measurement with PBS with few differences; the baseline of human serum is higher than PBS, which might cause by a number of proteins in human serum. However, the dynamic range of SERS-ICA is 0.01–100 ng/mL.

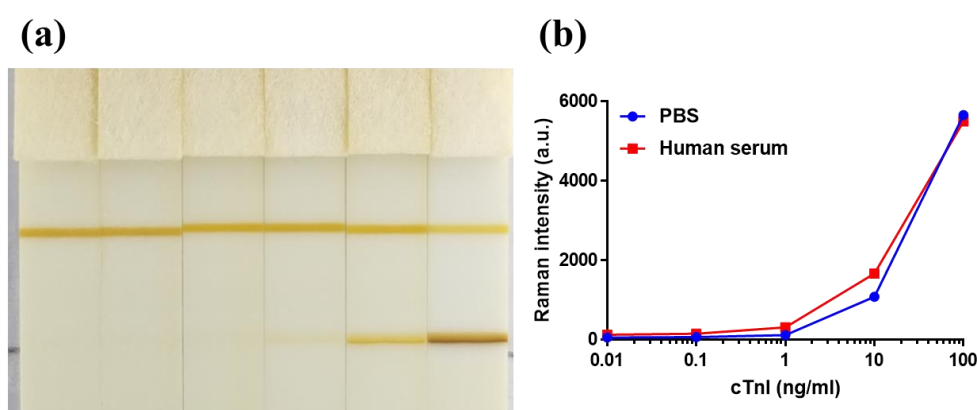


Figure 5. Human serum test. (a) Optical image of ICA strips reacted with 0–100 ng/mL cTnI in 10% human serum; (b) Optical and Raman analysis of the cTnI detection.

4. Conclusions

SERS-based ICA is a cheap, rapid, and bimodal diagnostic platform for AMI by measuring cTnI within 15 min. The bimodal analysis can be chosen by the situation. An optical analysis is preferable in urgent condition because its dynamic range includes clinical cut-off level of bad prognosis. Raman analysis is applicable for detailed and sensitive quantification of cTnI level but needed extra 5 min and Raman device. SERS-ICA is a versatile bimodal platform that can be applied to various biomarkers related to acute diseases.

Supplementary Materials: The following are available online at www.mdpi.com/xxx/s1, Figure S1: Optical image analysis with blue and green splits. Figure S2: Optical images of each seed growth step of SERS tags, Figure S3: Raman spectra of SERS tags with different laser, Figure S4: Raman intensity of different laser and power.

Author Contributions: Conceptualization, methodology, validation, data curation, writing—original draft preparation, visualization, I.K.; investigation, resources, E.S.; writing—review and editing,

supervision, project administration, C.J. and S.P.; funding acquisition, S.P. All authors have read and agreed to the published version of the manuscript.

Funding: This work was financially supported by the Technology Innovation Program (Project No. 20009092) funded by the Ministry of Trade, Industry, and Energy (MOTIE, South Korea).

Data Availability Statement: All the data were generated during the study.

Conflicts of Interest: The authors declare no conflict of interest. The funders had no role in the design of the study; in the collection, analyses, or interpretation of data; in the writing of the manuscript, or in the decision to publish the results.

References

1. Reed, G.W.; Rossi, J.E.; Cannon, C.P. Acute myocardial infarction. *Lancet* **2017**, *389*, 197–210. [https://doi.org/10.1016/S0140-6736\(16\)30677-8](https://doi.org/10.1016/S0140-6736(16)30677-8).
2. Davies, M.J.; Thomas, A.C. Plaque fissuring--the cause of acute myocardial infarction, sudden ischaemic death, and crescendo angina. *Br. Heart J.* **1985**, *53*, 363–373. <https://doi.org/10.1136/hrt.53.4.363>.
3. Chan, D.; Ng, L.L. Biomarkers in acute myocardial infarction. *BMC Med.* **2010**, *8*, 34. <https://doi.org/10.1186/1741-7015-8-34>.
4. Neumann, J.T.; Sørensen, N.A.; Ojeda, F.; Renné, T.; Schnabel, R.B.; Zeller, T.; Karakas, M.; Blankenberg, S.; Westermann, D. Early diagnosis of acute myocardial infarction using high-sensitivity troponin I. *PLoS ONE* **2017**, *12*, e0174288. <https://doi.org/10.1371/journal.pone.0174288>.
5. Javed, U.; Aftab, W.; Ambrose, J.A.; Wessel, R.J.; Mouanoutoua, M.; Huang, G.; Barua, R.S.; Weilert, M.; Sy, F.; Thatai, D. Frequency of Elevated Troponin I and Diagnosis of Acute Myocardial Infarction. *Am. J. Cardiol.* **2009**, *104*, 9–13. <https://doi.org/10.1016/j.amjcard.2009.03.003>.
6. O'Gara, P.T.; Kushner, F.G.; Ascheim, D.D.; Casey, D.E.; Chung, M.K.; Lemos, J.A.d.; Ettinger, S.M.; Fang, J.C.; Fesmire, F.M.; Franklin, B.A.; et al. 2013 ACCF/AHA Guideline for the Management of ST-Elevation Myocardial Infarction. *Circulation* **2013**, *127*, e362–e425, doi:doi:10.1161/CIR.0b013e3182742cf6.
7. Liu, M.; Jiang, R.; Zheng, M.; Li, M.; Yu, Q.; Zhu, H.; Guo, H.; Sun, H. A sensitive ratiometric biosensor for determination cardiac troponin I of myocardial infarction markers based on N, Zn-GQDs. *Talanta* **2022**, *249*, 123577. <https://doi.org/10.1016/j.talanta.2022.123577>.
8. Lim, J.Y.; Lee, S.S. Quartz crystal microbalance cardiac Troponin I immunosensors employing signal amplification with TiO₂ nanoparticle photocatalyst. *Talanta* **2021**, *228*, 122233. <https://doi.org/10.1016/j.talanta.2021.122233>.
9. Wen, R.; Zhou, C.; Tian, J.; Lu, J. Confined catalysis of MOF-818 nanozyme and colorimetric aptasensing for cardiac troponin I. *Talanta* **2023**, *252*, 123830. <https://doi.org/10.1016/j.talanta.2022.123830>.
10. Park, J.-H.; Park, E.-K.; Cho, Y.K.; Shin, I.-S.; Lee, H. Normalizing the Optical Signal Enables Robust Assays with Lateral Flow Biosensors. *ACS Omega* **2022**, *7*, 17723–17731. <https://doi.org/10.1021/acsomega.2c00793>.
11. Lim, W.; Qushmaq, I.; Cook, D.J.; Crowther, M.A.; Heels-Ansdell, D.; Devereaux, P.J. Elevated troponin and myocardial infarction in the intensive care unit: A prospective study. *Crit. Care* **2005**, *9*, R636–R644. <https://doi.org/10.1186/cc3816>.
12. Hwang, J.; Lee, S.; Choo, J. Application of a SERS-based lateral flow immunoassay strip for the rapid and sensitive detection of staphylococcal enterotoxin B. *Nanoscale* **2016**, *8*, 11418–11425. <https://doi.org/10.1039/C5NR07243C>.
13. Wuithschick, M.; Birnbaum, A.; Witte, S.; Sztucki, M.; Vainio, U.; Pinna, N.; Rademann, K.; Emmerling, F.; Kraehnert, R.; Polte, J. Turkevich in New Robes: Key Questions Answered for the Most Common Gold Nanoparticle Synthesis. *ACS Nano* **2015**, *9*, 7052–7071. <https://doi.org/10.1021/acsnano.5b01579>.
14. Lin, L.; Gu, H.; Ye, J. Plasmonic multi-shell nanomatryoshka particles as highly tunable SERS tags with built-in reporters. *Chem. Commun.* **2015**, *51*, 17740–17743. <https://doi.org/10.1039/C5CC06599B>.
15. Parolo, C.; Sena-Torralba, A.; Bergua, J.F.; Calucho, E.; Fuentes-Chust, C.; Hu, L.; Rivas, L.; Álvarez-Diduk, R.; Nguyen, E.P.; Cinti, S.; et al. Tutorial: Design and fabrication of nanoparticle-based lateral-flow immunoassays. *Nat. Protoc.* **2020**, *15*, 3788–3816. <https://doi.org/10.1038/s41596-020-0357-x>.
16. Benz, F.; Chikkaraddy, R.; Salmon, A.; Ohadi, H.; de Nijs, B.; Mertens, J.; Carnegie, C.; Bowman, R.W.; Baumberg, J.J. SERS of Individual Nanoparticles on a Mirror: Size Does Matter, but so Does Shape. *J. Phys. Chem. Lett.* **2016**, *7*, 2264–2269. <https://doi.org/10.1021/acs.jpcllett.6b00986>.
17. Saha, A.; Khalkho, B.R.; Deb, M.K. Au–Ag core–shell composite nanoparticles as a selective and sensitive plasmonic chemical probe for l-cysteine detection in Lens culinaris (lentils). *RSC Adv.* **2021**, *11*, 20380–20390. <https://doi.org/10.1039/D1RA01824H>.

Disclaimer/Publisher's Note: The statements, opinions and data contained in all publications are solely those of the individual author(s) and contributor(s) and not of MDPI and/or the editor(s). MDPI and/or the editor(s) disclaim responsibility for any injury to people or property resulting from any ideas, methods, instructions or products referred to in the content.